

Electrochemical and IR Spectroelectrochemical Investigations of the Series $\text{Mo}(\text{CO})_{6-n}(\text{CNR})_n$ ($n = 1-6$) ($\text{R} = 2,6\text{-Dimethylphenyl}$): *In Situ* Observation of *fac-mer* and *cis-trans* Isomerizations

Leslie J. Lyons* and Stephanie L. Pitz

Department of Chemistry, Grinnell College, Grinnell, Iowa 50112

David C. Boyd

Department of Chemistry, University of St. Thomas, St. Paul, Minnesota 55105

Received October 28, 1993[⊗]

Cyclic voltammetry and IR spectroelectrochemistry on the series of compounds $\text{Mo}(\text{CO})_{6-n}(\text{dmpi})_n$, where $\text{dmpi} = 2,6\text{-dimethylphenyl isocyanide}$ and $n = 1-6$, have determined the $E_{1/2}$ values for the first oxidation of the molybdenum isocyanides and the identity of the cation formed. The $\text{Mo}(\text{CO})_{6-n}(\text{dmpi})_n$ complexes undergo one-electron oxidation reactions at progressively less positive values as the substitution of isocyanides is increased. $\text{Mo}(\text{CO})_5(\text{dmpi})$ is oxidized at 1.18 V vs NHE while at the other extreme $\text{Mo}(\text{dmpi})_6$ is oxidized at -0.34 V vs NHE. An electrochemical ligand parameter, E_L , of 0.43 V has been calculated for the dmpi ligand. Stability of the oxidized products, $[\text{Mo}(\text{CO})_{6-n}(\text{dmpi})_n]^+$, also varies with substitution. Oxidation of the $n = 5$ and 6 compounds is chemically reversible, and IR spectroelectrochemistry indicates a stable $\text{Mo}(\text{I})$ species is formed. Two members of the series, *fac*- $\text{Mo}(\text{CO})_3(\text{dmpi})_3$ and *cis*- $\text{Mo}(\text{CO})_2(\text{dmpi})_4$, undergo electron transfer induced isomerizations upon oxidation by one electron. The isomerization reactions were confirmed by digital simulation of the cyclic voltammograms and IR spectroelectrochemical studies, which show clear conversion of the isomers upon electrolysis. The rate constants for the isomerization reactions range from 7.0 s^{-1} for the *fac*- $[\text{Mo}(\text{CO})_3(\text{dmpi})_3]^+ \rightarrow \text{mer}-[\text{Mo}(\text{CO})_3(\text{dmpi})_3]^+$ isomerization to 0.093 s^{-1} for the *cis*- $[\text{Mo}(\text{CO})_2(\text{dmpi})_4]^+ \rightarrow \text{trans}-[\text{Mo}(\text{CO})_2(\text{dmpi})_4]^+$ reaction. The $n = 1$ and 2 cations are short-lived and decompose to free ligands.

Introduction

Investigations of the effect of ligand substitution on electrochemical properties have been a theme of inorganic research for several decades and were recently the subject of an international symposium.¹ Early studies on chromium² and manganese³ coordination complexes have demonstrated the principle of ligand additivity initially developed by Bursten⁴ and subsequently quantified by Lever⁵ into a ligand electrochemical series. More recent studies on ruthenium,⁶ osmium,⁷ rhenium,⁸ cobalt,⁹ and zinc⁹ complexes have demonstrated that the ligand additivity principle applies to a broad range of transition metal complexes.

Another theme in electrochemical studies of inorganic complexes has been the observation of isomerization reactions which accompany oxidation or reduction reactions. The early focus in these investigations was the generation of 17-electron species. For example, Bond, Grabaric, and Jackowski¹⁰ generated the 17-electron cations *cis*- $[\text{M}(\text{CO})_2(\text{P-P})_2]^+$ (P-P is a chelating diphosphine ligand) and determined the rates of isomerization for the *trans* \rightarrow *cis* and *cis*⁺ \rightarrow *trans*⁺ reactions. Later studies¹¹ examined the effect of the structural isomerization reaction on the rate of electron transfer. Similar behavior has been observed for *fac-mer* isomerizations in the molybdenum complexes $\text{Mo}(\text{CO})_3\text{P}_3$ (where P is a phosphine ligand).¹² The preference for geometric isomers in different oxidation states has also been reported for ruthenium complexes with a mixture of sulfur and phosphine ligands.¹³

In this paper both these themes will be discussed within the context of electrochemical and infrared spectroelectrochemical

[⊗] Abstract published in *Advance ACS Abstracts*, November 15, 1994.

- (1) *Molecular Electrochemistry of Inorganic, Bioinorganic and Organometallic Compounds*; Pombeiro, A. J. L., McCleverty, J. A., Eds.; Proceedings of the NATO Advanced Research Workshop on Molecular Electrochemistry of Inorganic, Bioinorganic and Organometallic Compounds; Kluwer Academic Publishers: Dordrecht, The Netherlands, 1993.
- (2) Conner, J. A.; Jones, E. M.; McEwen, G. K.; Lloyd, M. K.; McCleverty, J. A. *J. Chem. Soc., Dalton Trans.* **1972**, 1246. (b) Treichel, P. M.; Essenmacher, G. J. *Inorg. Chem.* **1976**, *15*, 146.
- (3) Treichel, P. M.; Direen, G. E.; Mueh, H. J. *J. Organomet. Chem.* **1972**, *44*, 339. (b) Treichel, P. M. *Adv. Organometal. Chem.* **1973**, *11*, 21. (c) Treichel, P. M.; Mueh, H. J.; Bursten, B. E. *Isr. J. Chem.* **1977**, *15*, 253. (d) Treichel, P. M.; Firsich, D. W.; Essenmacher, G. P. *Inorg. Chem.* **1979**, *18*, 2405.
- (4) Bursten, B. E.; Green, M. R. *Prog. Inorg. Chem.* **1988**, *36*, 393.
- (5) Dodsworth, E. S.; Vleck, A. A.; Lever, A. B. *Inorg. Chem.* **1994**, *33*, 1045. (b) Lever, A. B. *Inorg. Chem.* **1990**, *29*, 1271.
- (6) Masui, H.; Lever, A. B. P.; Dodsworth, E. S. *Inorg. Chem.* **1993**, *32*, 258. (b) Auburn, P. R.; Dodsworth, E. S.; Haga, M. Liu; W. Nevin, W. A.; Lever, A. B. P. *Inorg. Chem.* **1991**, *30*, 3502. (c) Duff, C. M.; Heath, G. A. *Inorg. Chem.* **1991**, *30*, 2528. (d) Duff, C. M.; Heath, G. A. *J. Chem. Soc., Dalton Trans.* **1991**, 2401.

- (7) Heath, G. A.; Humphrey, D. G. In *Molecular Electrochemistry of Inorganic, Bioinorganic and Organometallic Compounds*; Pombeiro, A. J. L., McCleverty, J. A., Eds.; Proceedings of the NATO Advanced Research Workshop on Molecular Electrochemistry of Inorganic, Bioinorganic and Organometallic Compounds; Kluwer Academic Publishers: Dordrecht, The Netherlands, 1993; pp 589–593. (b) Heath, G. A.; Humphrey, D. G. *J. Chem. Soc., Chem. Commun.* **1991**, 1668.
- (8) Holder, G. N.; Bottomley, L. A. *Transition Met. Chem.* **1991**, *16*, 579. (b) Lever, A. B. P. *Inorg. Chem.* **1991**, *30*, 1980.
- (9) Lever, A. B. P. *Inorg. Chim. Acta* **1993**, *203*, 171.
- (10) Bond, A. M.; Grabaric, B. S.; Jackowski, J. J. *Inorg. Chem.* **1978**, *17*, 2153.
- (11) Bond, A. M.; Darensbourg, D. J.; Mocellin, E.; Stewart, B. J. *J. Am. Chem. Soc.* **1981**, *103*, 6827.
- (12) Bond, A. M.; Carr, S. W.; Colton, R. *Organometallics* **1984**, *3*, 541.
- (13) Bag, N.; Lahiri, G. K.; Chakravorty, A. *J. Chem. Soc., Dalton Trans.* **1990**, 1557.

results on the series of compounds Mo(CO)_{6-n}(dmpi)_n where $n = 1-6$ and dmpi = 2,6-dimethylphenyl isocyanide. The cyclic voltammetric results for the series of complexes display the expected ligand additivity behavior allowing calculation of the ligand electrochemical parameter, E_L , for 2,6-dimethylphenyl isocyanide. The complexes also display the full range of chemical reversibility upon oxidation by one electron, including geometric isomerizations. The synthetic route to the entire series of molybdenum isocyanides was developed by Albers and Coville¹⁴ previously, and this synthetic route was utilized by Minelli and Maley¹⁵ in their investigation of the ⁹⁵Mo NMR chemical shifts of the complexes. We were originally interested in the trend in electrochemical properties over this series and then discovered that two members of the series, $n = 3$ and 4, undergo electron transfer induced isomerizations upon oxidation. The isomerization reactions were further studied using infrared spectroelectrochemistry and modeled by digitally simulating the cyclic voltammograms. The trends in the electrochemical properties and ⁹⁵Mo chemical shifts were further analyzed with molecular mechanics and molecular orbital calculations.

Experimental Section

Synthesis and Characterization. All compounds were synthesized using the method described by Albers and Coville.¹⁴ The syntheses were performed under argon using dichloromethane that was dried and distilled over P₂O₅ prior to use. Mo(CO)₆, 2,6-dimethylphenyl isocyanide (dmpi), and PdO were used as received from Aldrich Chemical. The products were purified by recrystallization from CH₂Cl₂ and hexane and stored at -5 °C in a drybox. The identities of all the compounds were verified by comparing ⁹⁵Mo NMR and IR data to previously published results.¹⁵ NMR data were acquired on a Bruker AC 300 MHz spectrometer fit with a 10 mm broad band probe (¹⁰⁹Ag-³¹P). The ⁹⁵Mo NMR data (reported in ppm) were acquired at 19.560 MHz and referenced to an external standard of 2 M Na₂MoO₄ in basic D₂O. IR spectra were measured on a Nicolet 5XSB FT-IR spectrometer as KBr pellets.

Cyclic Voltammetry. All experiments were performed under a nitrogen atmosphere at room temperature (24 °C) using a 2 mm glassy carbon disk working electrode which was polished with 0.30 μm alumina and sonicated prior to use. A platinum coil acted as the counter electrode, and the reference was a cadmium/mercury amalgam non-aqueous reference electrode.¹⁶ The tabulated potentials have also been scaled to the normal hydrogen reference electrode (NHE). Positive feedback *i*R compensation was used in all experiments. Since dichloromethane is a very resistive solvent, it was particularly important to compensate for all solution resistance between the working and reference electrodes. The value for the feedback resistance was determined by potentiostatic oscillation. Slow scan rate studies ($v < 2$ V/s) were performed on a PAR 173 potentiostat using a PAR 175 universal programmer to generate the cyclic wave forms and output to a X-Y chart recorder. Fast scan rate studies for Mo(CO)₅(dmpi) were performed using the PAR 173 and 175 interfaced to a Nicolet digital oscilloscope and a 1 mm glassy carbon disk working electrode. Voltammetric data for digital simulations were acquired on an EG&G PAR Model 273 potentiostat/galvanostat interfaced to a personal computer running the EG&G PAR Model 270 electrochemical software. The analyte solution consisted of 6–8 mM molybdenum complex and 0.10 M tetrabutylammonium tetrafluoroborate (Southwestern Analytical, used as received) in freshly distilled CH₂Cl₂. Dry alumina was added to the solution of Mo(CO)₅(dmpi) to extend the potential window to more positive values. Cyclic voltammograms of each compound were performed at scan rates of 10, 20, 50, 100, 200, 500, and 1000 mV/s. Additionally, voltammograms of Mo(CO)₅(dmpi) were acquired up to 20 V/s. Replicate experiments on different synthetic batches were performed to ensure reproducibility. Ferrocene was added to each solution as an internal standard just prior to the completion of the

experiment. Under these conditions, ferrocene displays a $E_{1/2}$ of 1.21 V vs Cd/Hg and a peak separation (ΔE_p) of 60 mV up to a scan rate of 1.0 V/s.

Digital Simulation. Simulations were performed using the explicit finite difference method of Feldberg.¹⁷ Pascal simulation programs were run on an AST 286 computer with additional memory and a math coprocessor. The mechanism simulated was a typical square scheme with two electron transfer steps connected to each other by two chemical steps. Simulations were run both with and without a solution electron transfer reaction (cross reaction). Each electron transfer step was treated as quasi-reversible with the formal potential E° , electron-transfer coefficient α , and standard heterogeneous electron transfer rate parameter ψ values initially determined from the experimental voltammograms and then modified to fit the experimental data. The diffusion coefficients of the four species in the square scheme were assumed to be equal. The pseudo-first-order chemical rate constants were determined by trial and error to fit the data over at least a decade variation in scan rate.

Spectroelectrochemistry. Approximately 2 mM solutions of the molybdenum isocyanide compounds with 0.5 M tetrabutylammonium hexafluorophosphate as the electrolyte were prepared in CH₂Cl₂, which was dried and distilled over P₂O₅ and stored over alumina. This solution was syringed into an airtight custom-made IR spectroelectrochemical cell¹⁸ with a platinum disk working electrode, a platinum wire counter electrode, and platinum wire pseudo-reference electrode connected to an ElectroSynthesis Corp. (ESC) Model 410 potentiostatic controller with an ESC Model 420-A accessory power unit. The cell was placed into a Laser Precision Analytical RFX-40 FTIR. Data was acquired using a Laser Precision Analytical personal computer. IR spectra were measured at a fixed potential at intervals of 30 s. The potential used was approximately 200 mV more positive of the half-wave potential of the complex to ensure complete electrolysis of the thin layer solution.

Molecular Orbital Calculations. The HOMO energies were calculated on a Macintosh Quadra 700 computer using CAChe software. Molecular geometries were minimized by allowing for sequential rotation around the isocyanide–molybdenum bonds in each complex. Extended Huckel calculations were performed on each member of the series using a Wolfberg–Helmholtz parameter of 1.75 and STO-3G basis set resulting in the energy and molecular orbital surface of the HOMO.

Results and Discussion

Cyclic Voltammetry. The cyclic voltammograms of the molybdenum substitution series display interesting thermodynamic and kinetic behavior as a function of ligand substitution. The $E_{1/2}$ values and the chemical reversibility of the voltammetry, hence the stability of the monocations, vary systematically with the composition of the ligands. Variable scan rate cyclic voltammograms were performed on each member of the series Mo(CO)_{6-n}(dmpi)_n ($n = 1-6$). For the $n = 5$ and 6 members of the series chemically and electrochemically reversible (Nernstian) behavior was observed for the oxidation to the monocation [Mo(CO)_{6-n}(dmpi)_n]⁺ ($n = 5$ and 6) (see Figure 1). For both of these compounds a plot of i_{pa} vs $v^{1/2}$ was linear, ΔE_p was 60 mV and did not increase with increasing scan rates, and the ratio of the anodic and cathodic currents (i_{pa}/i_{pc}) was unity. These results agree with previous studies on the oxidation of Mo(dmpi)₆ in which a stable monocation was observed which was subsequently oxidized to the dication [Mo(dmpi)₆]²⁺. In the presence of additional ligand, the dication then undergoes a chemical reaction to form the seven-coordinate species [Mo(dmpi)₇]²⁺, which has been extensively studied by Walton *et al.*¹⁹

Voltammetric studies on the $n = 1-4$ compounds deviated from the Nernstian behavior displayed by the more fully

(14) Albers, M. O.; Coville, N. J. *Inorg. Chim. Acta* **1982**, *65*, L7–L8.

(15) Minelli, M.; Maley, W. J. *Inorg. Chem.* **1989**, *28*, 2954–2958.

(16) Hall, J. L.; Jennings, P. W. *Anal. Chem.* **1976**, *48*, 2026–2027.

(17) Feldberg, S. W. In *Electroanalytical Chemistry*; Bard, A. J., Ed.; Marcel Dekker: New York, 1969; Vol. 3, pp 199–296.

(18) Bullock, J. P.; Mann, K. R. *Inorg. Chem.* **1989**, *28*, 4006 and references therein.

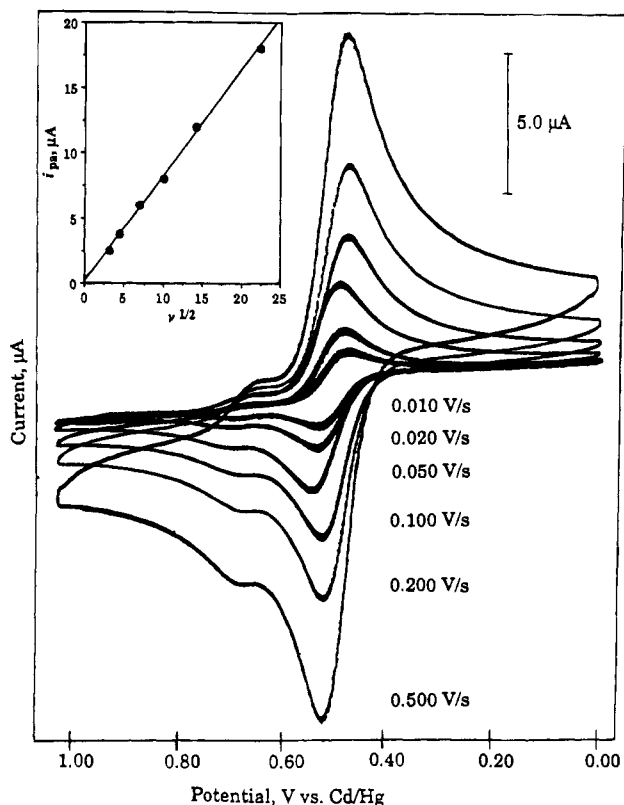


Figure 1. Variable scan rate cyclic voltammograms of $\text{Mo}(\text{dmpe})_6$ in 0.10 M $(\text{TBA})\text{BF}_4$ and CH_2Cl_2 at a glassy carbon disk working electrode versus a Cd/Hg reference electrode. The inset graph is a plot of i_{pa} vs $v^{1/2}$ and is typical of the Nernstian behavior displayed by the $n = 5$ and $n = 6$ molybdenum complexes.

substituted compounds. For $\text{cis-Mo}(\text{CO})_4(\text{dmpe})_2$ the ratio of the anodic and cathodic currents was far from unity (see Figure 2). Voltammograms at scan rates faster than 500 mV/s were necessary to observe chemical reversibility. The scan rate dependence of the peak current ratios is indicative of a chemical reaction proceeding after the electron transfer reaction, an EC process ($E = \text{electrochemical step}$, $C = \text{chemical step}$). The $\text{Mo}(\text{CO})_5(\text{dmpe})$ oxidation was chemically irreversible up to scan rates of 20 V/s at which a small cathodic current was observed on the return sweep, allowing calculation of the $E_{1/2}$ for the oxidation reaction.

Successive cyclic voltammograms of the $\text{fac-Mo}(\text{CO})_3(\text{dmpe})_3$ and $\text{cis-Mo}(\text{CO})_2(\text{dmpe})_4$ compounds indicated the presence of a second electroactive species in solution. We believe that these complexes undergo electrochemically induced isomerization reactions similar to observations on other transition metal species.^{10,11} This hypothesis is supported by Figure 3 in which two sequential voltammetric scans are presented for the oxidation of $\text{fac-Mo}(\text{CO})_3(\text{dmpe})_3$. In the first scan of the cyclic voltammogram, only one anodic peak is observed at 1.51 V vs Cd/Hg, while, on the return scan, two cathodic peaks are observed at 1.43 and 1.27 V vs Cd/Hg. The second anodic sweep has two anodic peaks with a new peak at 1.36 V vs Cd/Hg. We have assigned the first species, on the basis of its IR spectrum, as the *fac* isomer and the new species, which is easier to oxidize, as the *mer* isomer. Bond *et al.* observed similar behavior in the series of compounds $\text{Mo}(\text{CO})_3\text{P}_3$ ($\text{P} = \text{PMe}_2\text{-Ph}$, P(OPh)_3 , P(OMe)_3 , $\text{P(OMe)}_2\text{Ph}$, P(OMe)Ph_2 , $\text{PPh}_2(\text{CH}_2\text{Ph})$)

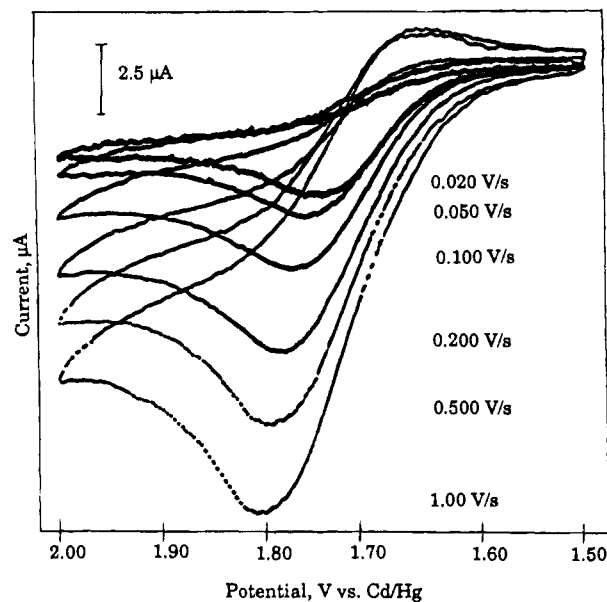


Figure 2. Variable scan rate cyclic voltammograms of $\text{cis-Mo}(\text{CO})_4(\text{dmpe})_2$ in 0.10 M $(\text{TBA})\text{BF}_4$ and CH_2Cl_2 at a glassy carbon disk working electrode versus a Cd/Hg reference electrode. The chemical irreversibility is typical of the $n = 1$ and $n = 2$ molybdenum complexes.

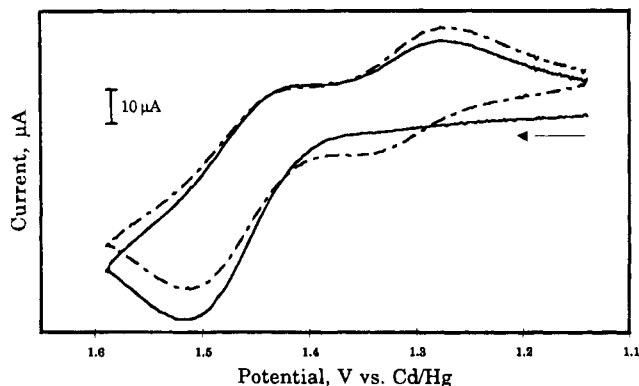


Figure 3. Successive oxidative cyclic voltammograms of 8 mM *fac-Mo*(CO) $_3$ (dmpe) $_3$ in 0.10 M $(\text{TBA})\text{BF}_4$ and CH_2Cl_2 at a glassy carbon disk working electrode versus a Cd/Hg reference electrode and at a scan rate of 1.0 V/s. The second cycle is the dotted line. The arrow indicates the origin of the scan and the scan direction.

also observing the *mer* isomer to be more easily oxidized than the *fac*.¹¹ Similar behavior is observed for the oxidation of $\text{Mo}(\text{CO})_2(\text{dmpe})_4$ with the assignment of *cis* to the parent isomer and *trans* to the electrochemically produced isomer. In a related system, Bond and Darensbourg also described the electrochemistry of $\text{Mo}(\text{CO})_4(\text{P}(\text{nBu})_3)_2$ by including both isomers.¹¹ In order to verify the electrochemically induced isomerization reactions, digital simulation of the proposed mechanism and infrared spectroelectrochemistry were employed as described below.

From the cyclic voltammetric studies, the $E_{1/2}$ values for the oxidation reaction of each member of the $\text{Mo}(\text{CO})_{6-n}(\text{dmpe})_n$ series were determined (see Table 1). In addition, the $E_{1/2}$ values for the two isomers of $\text{Mo}(\text{CO})_3(\text{dmpe})_3$ (*mer/fac*) and $\text{Mo}(\text{CO})_2(\text{dmpe})_4$ (*cis/trans*) were also determined. The $E_{1/2}$ values decrease with increasing *dmpe* substitution, as one would expect from the increasing electron-donating ability of the *dmpe* ligands compared to the carbonyl ligands. Each *dmpe* substitution for a carbonyl ligand makes the complex easier to oxidize by approximately 200 mV. The *trans-Mo*(CO) $_2$ (dmpe) $_4$ isomer is easier to oxidize than the *cis*, and the *mer-Mo*(CO) $_3$ (dmpe) $_3$ is easier to oxidize than the *fac*. The effect of the geometric

(19) Klendworth, D. D.; Welters, W. W., III; Walton, R. A. *Organometallics* **1982**, *1*, 336. (b) Mialki, W. S.; Wild, R. E.; Walton, R. A. *Inorg. Chem.* **1981**, *20*, 1380. (c) Klendworth, D. D.; Welters, W. W., III; Walton, R. A. *J. Organomet. Chem.* **1981**, *213*, C13.

Table 1. Physical Properties of Mo(CO)_{6-n}(dmpi)_n

<i>n</i>	color	$\delta(^{95}\text{Mo})^a$ (ppm)	IR bands ^b (cm ⁻¹)		$E_{1/2}^c$ (V vs Cd/Hg)	$E_{1/2}^c$ (V vs NHE)	HOMO energy (eV)	ΣE_L^e (V vs NHE)
			CN	CO				
1	ivory	-1848	CN CO	2091 2062 1982	2.08 ^d	1.18	-10.28	5.38
2	pale yellow	-1824	CN CO	2140 2097 2011 1929 1897	1.78	0.88	-10.19	4.82
3	bright yellow	-1785	CN CO	2134 2069 1936 1900 1872	<i>fac</i> = 1.48 <i>mer</i> = 1.32	<i>fac</i> = 0.58 <i>mer</i> = 0.42	-10.18 -10.00	4.26 ^f 4.26 ^f
4	brown-orange	-1711	CN CO	2117 2018 1986 1936 1889 1857	<i>cis</i> = 1.07 <i>trans</i> = 0.92	<i>cis</i> = 0.17 <i>trans</i> = 0.02	-10.08 -9.97	3.70 ^f 3.70 ^f
5	bright orange	-1625	CN CO	2020 1995 1950 1860	0.70	0.20	-9.94	3.14
6	red-orange	-1526	CN	2015 1935	0.56	0.34	-9.90	2.58

^aAgainst the external standard Na₂MoO₄ in basic D₂O. ^bMeasured as KBr pellets. When isomers are possible, the assignments are for the synthesized isomer, *cis* for *n* = 2, *fac* for *n* = 3, and *cis* for *n* = 4. ^cPotentials were measured versus the Cd/Hg nonaqueous reference electrode and are also reported scaled to the normal hydrogen electrode (NHE) using the potential for the ferrocene 0/+ couple as an internal standard. ^dAcquired at 20 V/s using a 1 mm glassy carbon disk working electrode. ^eCalculated as in ref 5b. ^fAssuming no geometric correction for stabilization by π ligands.

arrangement of the ligands on the $E_{1/2}$ values can best be understood by examining the HOMO orbital which is discussed below. Since the $E_{1/2}$ value was measured for [Mo(dmpi)₆]^{0/+}, it is possible to apply Lever's ligand parametrization model to these data to calculate a ligand electrochemical parameter, E_L , for dmpi and to analyze the electrochemical potentials for the entire series using Lever's quantitative approach.⁵ On the basis of the examination of the oxidation data for 480 complexes, Lever has developed a general relationship for ligand additivity which states

$$E_{\text{calc}} = S_M[\sum E_L(L)] + I_M$$

Relevant to our study, he reports values for S_M and I_M for the oxidation of Mo(0) to Mo(I) on the basis of data for 24 molybdenum complexes from the literature. Using his values of $S_M = 0.74 \pm 0.03$ and $I_M = -2.25 \pm 0.10$, we can calculate E_L for dmpi from our observed $E_{1/2}$ value for [Mo(dmpi)₆]^{0/+} scaled to the NHE reference electrode. The E_{dmpi} is

$$E_{\text{dmpi}} = (E_{1/2} - I_M)/(S_M \times 6) = [-0.34 \text{ V} - (-2.25)]/(0.74 \times 6) = 0.43 \text{ V}$$

This E_L value falls in the range predicted by Lever for isonitriles and falls between the E_L values for phenyl isocyanide ($E_L = 0.41$) and 2,6-dichloro isocyanide ($E_L = 0.46$). From E_{dmpi} and Lever's previous calculation for carbon monoxide, $E_{\text{CO}} = 0.99 \text{ V}$, we calculated the ΣE_L for the entire series of complexes and plotted these sums against the observed $E_{1/2}$ values (see Figure 4, filled circles). Our data are linear with a slope of 0.58, an intercept of -1.96, and a correlation coefficient of 0.97. The lower slope for our Mo(CO)_{6-n}(dmpi)_n series suggests the Mo(I) oxidation state is more stable in these complexes than in the 24 complexes (mostly phosphine- and amine-substituted carbonyl complexes) which were used to determine Lever's S_M . The intercept term has been interpreted

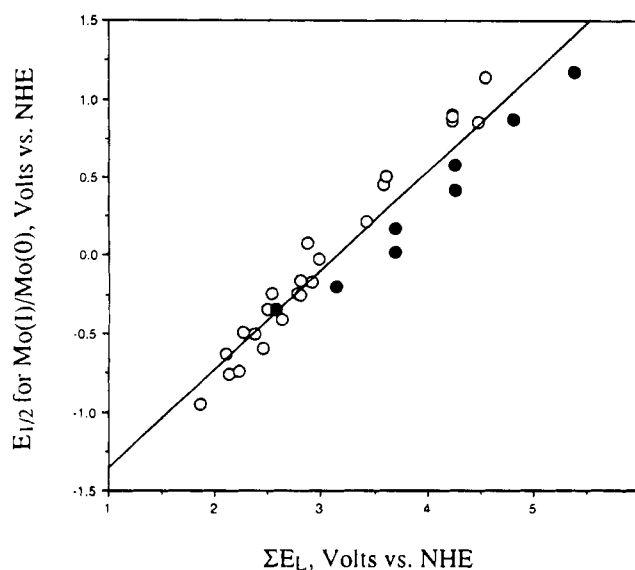


Figure 4. Correlation of the first oxidative $E_{1/2}$ (scaled to the NHE reference electrode) and the sum of the electrochemical ligand parameters, ΣE_L . The filled circles are for the Mo(CO)_{6-n}(dmpi)_n complexes, and the open circles are from Table 4 of ref 5b.

by Lever to include three contributions, *a*, *b*, and *c*, such that

$$I_M = a + nb + c$$

The *a* term is due to the ionization energy for Mo(I)/Mo(0) in the gas phase so that term should be the same for all 32 complexes. The *c* term includes solvation effects which seem to be negligible for the variety of organic solvents that Lever has examined. The *b* term is a spherical electrostatic term which accounts for the repulsion between the lone pair of the ligand and the metal d orbitals in crystal field theory. This term

contributes to I_M by the factor n , the number of ligands. We would expect the b term to vary with the ligand identity just as the d orbital splitting varies with ligand strength in the spectrochemical series, so our intercept value is dominated by this term and should be different for our isocyanide series. We observe linearity for our data similar to that of Lever. A plot of our isocyanide data with the 24 molybdenum complexes previously reported by Lever is shown in Figure 4. Our data extend the previous plot to higher $\sum E_L$; the linear regression for all 32 complexes decreases to 0.93.

In these complexes the $E_{1/2}$ values measure the electron density at the molybdenum-based HOMO as does ^{95}Mo NMR and there is a correlation of the half-wave potentials with the ^{95}Mo chemical shift. The ^{95}Mo chemical shift for $\text{Mo}(\text{CO})_5(\text{dmp})$ is -1848 ppm, the most shielded, and it is also the hardest to oxidize with an $E_{1/2}$ of 1.18 V vs NHE. Similarly, the ^{95}Mo chemical shift for $\text{Mo}(\text{dmp})_6$ is most deshielded at -1526 ppm and it is the easiest to oxidize with an $E_{1/2}$ of -0.34 V vs NHE. However, the correlation between ^{95}Mo chemical shift and the $E_{1/2}$ values is not linear.

Molecular Orbital Calculations. The HOMO energies calculated for each of the eight complexes correlate very well with the half-wave potentials and ^{95}Mo chemical shifts (see Table 1). In all of the complexes the HOMO is predominantly a metal-centered orbital of d character with D_{4h} symmetry. There are very small contributions from the carbons of the isocyanide ligands. The increasing electron density at the molybdenum as isocyanide substitution increases is confirmed by the calculations. $\text{Mo}(\text{dmp})_6$ has the highest HOMO energy, is the easiest to oxidize electrochemically, and is the most deshielded in the ^{95}Mo NMR. In particular, the relative HOMO energies agree with the observed $E_{1/2}$ values for the *fac-mer* $\text{Mo}(\text{CO})_3(\text{dmp})_3$ and *cis-trans* $\text{Mo}(\text{CO})_2(\text{dmp})_4$ isomers. The *mer* isomer has a higher HOMO energy and is easier to oxidize. Correspondingly, the *trans* HOMO energy is also higher, in agreement with the voltammetry data. The difference in $E_{1/2}$ for the isomeric pairs is due to the increased stabilization of the HOMO orbital by π bonding with the carbonyl ligands.^{3c} The HOMO is in the plane of the isocyanide ligands for the *trans*- $\text{Mo}(\text{CO})_2(\text{dmp})_4$ complex with no π -bonding interactions possible with the carbonyl ligands. In the *cis* complex the d orbital is stabilized by a π interaction with one carbonyl ligand; thus the *cis* isomer is more difficult to oxidize than the *trans*. Similarly in the $\text{Mo}(\text{CO})_3(\text{dmp})_3$ complexes, the d orbital is stabilized by interaction with one carbonyl ligand for the *mer* isomer while the *fac* isomer is stabilized by two carbonyls. The degree of stabilization by carbonyl ligands leads to the less positive $E_{1/2}$ for the *mer* complex relative to the *fac*.

Infrared Spectroelectrochemistry. The observation of an EC process for $\text{Mo}(\text{CO})_5(\text{dmp})$ and *cis*- $\text{Mo}(\text{CO})_4(\text{dmp})_2$ and an electrochemically induced isomerization for *fac*- $\text{Mo}(\text{CO})_3(\text{dmp})_3$ and *cis*- $\text{Mo}(\text{CO})_2(\text{dmp})_4$ led to further investigation of the products of the oxidation reactions by infrared spectroelectrochemistry. In this experiment the IR spectrum of the thin layer electrochemical solution was constantly monitored during bulk electrolysis of the solution.

The primary goal of the infrared spectroelectrochemical studies was to determine the identity of the new species formed upon oxidation of *fac*- $\text{Mo}(\text{CO})_3(\text{dmp})_3$ and *cis*- $\text{Mo}(\text{CO})_2(\text{dmp})_4$. Electrolysis of *fac*- $\text{Mo}(\text{CO})_3(\text{dmp})_3$ in the IR spectroelectrochemical cell resulted in a decrease in intensity of the two original carbonyl bands (1943 and 1890 cm^{-1}) and the two initial isocyanide bands (2133 and 2075 cm^{-1}) and the appearance of two new carbonyl bands (2013 and 1975 cm^{-1}) and three new isocyanide bands (2125 , 2012 , and 2060 cm^{-1}).

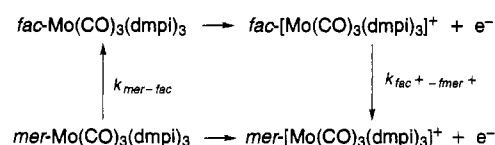
Observation of two carbonyl bands and two isocyanide bands in the original spectrum is consistent with the C_{3v} symmetry of the *fac* isomer of $\text{Mo}(\text{CO})_3(\text{dmp})_3$, while three new carbonyl and three new isocyanide bands are predicted for the C_{2v} *mer* symmetry. We did observe three new isocyanide bands as predicted by theory but only two carbonyl bands suggesting that two of the carbonyl bands are overlapping. The general shift of infrared carbonyl and isocyanide features to higher energy with increased metal oxidation state is expected due to a decrease in π^* orbital occupancy and decreased π back-bonding. There is not significant loss of material to decay or other chemical reactions as evidenced by the presence of isosbestic points maintained during the electrolysis, though the IR features of *mer*- $[\text{Mo}(\text{CO})_3(\text{dmp})_3]^+$ are less intense than those of *fac*- $\text{Mo}(\text{CO})_3(\text{dmp})_3$. The decreased band intensity is characteristic of this type of oxidation and has been discussed previously.¹⁸

Infrared spectroelectrochemistry also confirms the identity of the *trans* isomer formed upon oxidation of *cis*- $\text{Mo}(\text{CO})_2(\text{dmp})_4$ (Figure 5). The CO bands for the C_{2v} symmetry *cis* isomer at 1894 and 1860 cm^{-1} decrease during electrolysis, while a new CO band at 1944 cm^{-1} grows into the spectrum. Similarly, the isocyanide bands for the *cis* isomer at 2125 , 2045 , 2021 , and 1990 cm^{-1} decrease in intensity and one new band appears at 2094 cm^{-1} . The shift from four isocyanide bands and two carbonyl bands, characteristic of the C_{2v} symmetry *cis*- $\text{Mo}(\text{CO})_2(\text{dmp})_4$, to one isocyanide and one carbonyl band, consistent with the D_{4h} *trans* isomer confirms the proposed isomerization scheme. Again three isosbestic points indicate that the electrolysis produces only one product.

IR spectroelectrochemical studies on $\text{Mo}(\text{CO})(\text{dmp})_5$ and $\text{Mo}(\text{dmp})_6$ suggest that stable Mo(I) species of both of these are formed. This is in agreement with studies by Weaver and Walton on $[\text{Mo}(\text{dmp})_6]^+$.²⁰

For the $\text{Mo}(\text{CO})_5(\text{dmp})$ and $\text{Mo}(\text{CO})_4(\text{dmp})_2$ compounds, the Mo(I) species formed decompose to free ligands. Initially the bands shift to higher energy, as expected for formation of a cation, and then the bands diminish with the concomitant increase in free ligand bands. The decomposition process was so vigorous for $[\text{Mo}(\text{CO})_5(\text{dmp})]^+$ that fine bubbles were observed at the counter electrode, presumably due to CO evolution.

Scheme 1



Digital Simulation. The mechanism simulated was a typical square scheme, shown for *fac*- $\text{Mo}(\text{CO})_3(\text{dmp})_3$ in Scheme 1. Initially, the two neutral isomers were considered to be in equilibrium and the ratio of the isomers was described by the equilibrium constant $K_{\text{mer-fac}}$ where $K_{\text{mer-fac}} = [\text{mer}]/[\text{fac}]$. In this scheme the neutral *fac* isomer is oxidized to the cation *fac*⁺ which undergoes an isomerization reaction in solution to form *mer*⁺. The *mer*⁺ cation is reduced back to the *mer* neutral species at less positive potentials than the *fac*⁺ to *fac* reduction. In another solution isomerization reaction, the *mer* species is converted back to the *fac* species, regenerating the original isomer. A comparison of the experimental cyclic voltammogram and the simulation at 1.0 V/s is shown in Figure 6. The agreement is quite good with the best fit obtained when the *fac*

(20) Enger, S. K.; Weaver, M. J.; Walton, R. A. *Inorg. Chim. Acta* **1987**, *129*, L1-L3.

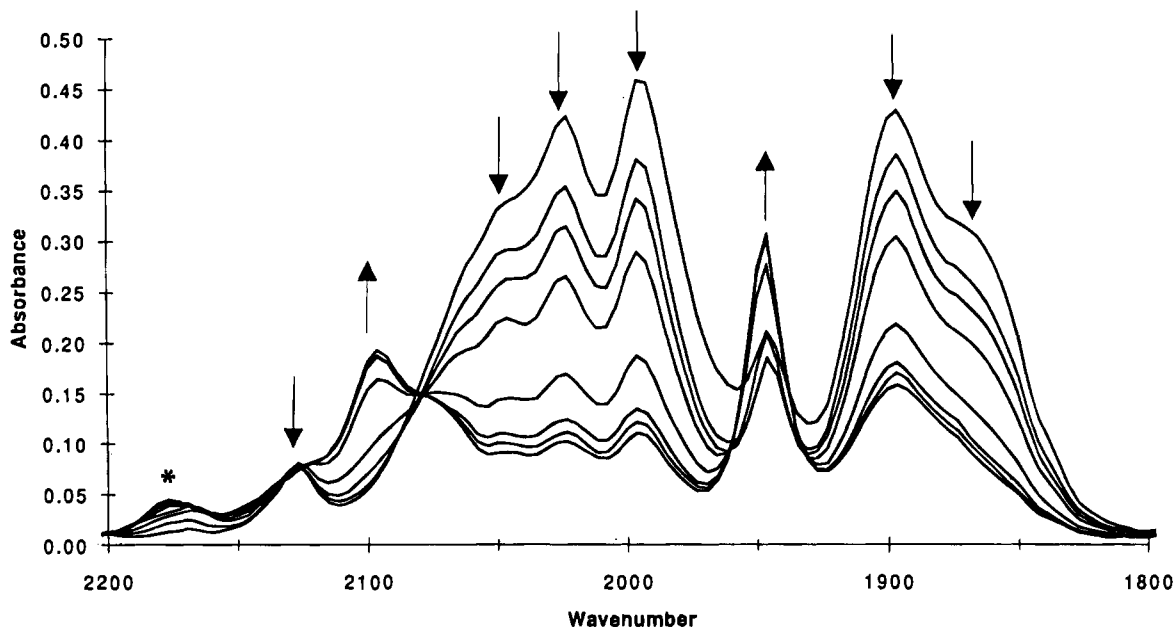


Figure 5. Infrared spectroelectrochemistry of 2 mM *cis*-Mo(CO)₂(dmpi)₄ in 0.5 M TBAPF₆ in CH₂Cl₂. Each infrared spectrum was acquired at 30 s intervals. The downward arrows indicate *cis*⁺ bands which decrease during the experiment while the up arrows indicate *trans*⁺ bands which grow in during the experiment. The asterisk indicates an impurity.

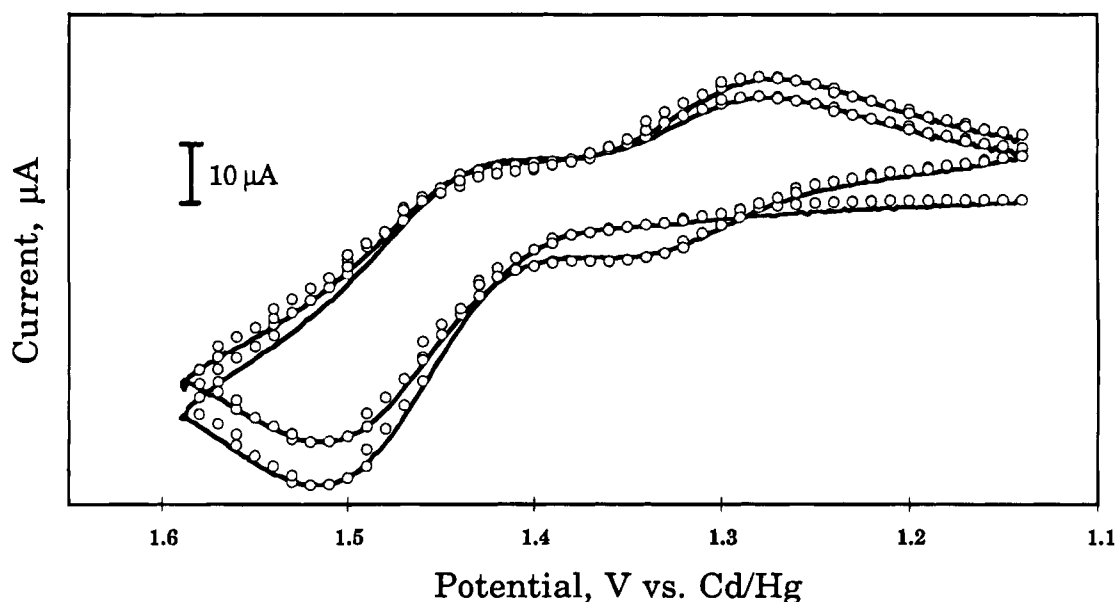


Figure 6. Comparison of the digital simulation (points) and experimental voltammogram (line) for the oxidation of *fac*-Mo(CO)₃(dmpi)₃ at 1.0 V/s. Simulation parameters are as follows: for the *fac* oxidation electron transfer reaction, $\alpha = 0.65$, $\psi = 0.50$, and $E^\circ = 1.48$ V; for the *mer* oxidation electron transfer reaction, $\alpha = 0.795$, $\psi = 0.80$, and $E^\circ = 1.32$ V. The solution isomerization reactions were simulated using ψ_k , $fac^+ - mer^+ = 0.18$ and ψ_k , $mer - fac = 0.0045$. ψ_k is related to the reaction rate constant, k_{reacn} , by the equation $k_{\text{reacn}} = \psi_k(38.92v)$ where v is the scan rate and $38.92 \text{ V}^{-1} = F/RT$. The equilibrium constant $K_{mer-fac} = 0.090$.

isomer is in equilibrium initially with 9% of the *mer* isomer. Simulations including the solution electron transfer reaction, $fac + mer^+ \rightarrow fac^+ + mer$, were run but gave the same results as simulations without the inclusion of the solution electron transfer reaction. Since the value of the equilibrium constant for the solution electron transfer reaction is quite small, 2.4×10^{-3} , the reaction would not be expected to change the solution concentrations near the electrode surface, as discussed by Evans.²¹ Vallat and Laviron have come to the same conclusion on the basis of an experimental study of the square scheme involving *cis/trans*-M(CO)₂(P-P)₂ and *cis/trans*-[M(CO)₂(P-P)₂]⁺ (P-P is a chelating phosphine ligand).²² The voltam-

metry of *cis*-Mo(CO)₂(dmpi)₄ was also simulated using a similar square scheme (Scheme 1) with *cis*-Mo(CO)₂(dmpi)₄ the parent isomer; however, the isomerization rates were much slower. At scan rates greater than 0.150 V/s, the *trans* isomer was not observed. Again inclusion of the solution electron transfer reaction, $cis + trans^+ \rightarrow cis^+ + trans$, had no effect on the simulation results and the equilibrium balance of neutral isomers was 97% *cis* and 3% *trans*.

From the simulation fits, the rate constants for the isomerization reactions and half-lives for the species were calculated to be as follows:

(21) Evans, D. H. *Chem. Rev.* **1990**, *90*, 744.

(22) Vallat, A.; Person, M.; Roullier, L.; Laviron, E. *Inorg. Chem.* **1987**, *26*, 332.

reaction	k , s ⁻¹
$fac-[Mo(CO)_3(dmpi)_3]^+ \rightarrow mer-[Mo(CO)_3(dmpi)_3]^+$	7.0 ± 1.4
$mer-Mo(CO)_3(dmpi)_3 \rightarrow fac-Mo(CO)_3(dmpi)_3$	0.78 ± 0.19
$cis-[Mo(CO)_2(dmpi)_4]^+ \rightarrow trans-[Mo(CO)_2(dmpi)_4]^+$	0.093 ± 0.006
$trans-Mo(CO)_2(dmpi)_4 \rightarrow cis-Mo(CO)_2(dmpi)_4$	0.14 ± 0.03

For $n = 3$, the cation isomerizes faster than the neutral complex but the neutral $n = 4$ *trans* complex isomerizes faster than than the *cis*⁺. The slow formation of the *trans* cation and the relatively fast isomerization of the neutral *trans* complex are borne out by the small amount of these species observed in the voltammetry. These rate constants are similar to published work. Bond, Grabaric, and Grabaric measured the rate constant for the isomerization of $fac-[Mn(CO)_3(L-L)X]^+$ to the *mer* cation to be 4.2 s^{-1} in CH_2Cl_2 and at $25^\circ C$ (L-L is a chelating ligand and X is a halide). They observed no solvent dependence for the isomerization and suggested a twist mechanism to be operating.²³ Bond, Grabaric, and Jackowski also measured rate constants for *cis*- $Mo(CO)_2(P-P)_2$ complexes (where P-P is a chelating phosphine ligand) which also undergo isomerization reactions in a square scheme.¹⁰ At $25^\circ C$ *cis*- $[Mo(CO)_2(P-P)_2]^+$ complexes isomerize with much faster rate constants of 20.5 s^{-1} for P-P = bis(diphenylphosphino)methane and 32.7 s^{-1} for P-P = 1,2-bis(diphenylphosphino)ethane while the *trans*- $Mo(CO)_2(dppe)_2$ complex isomerizes with a slower rate of 0.055 s^{-1} . Rate constants for the isomerization of *trans*- $Ru(ROCS_2)_2(PPh_3)_2$ to *cis*- $Ru(ROCS_2)_2(PPh_3)_2$ ($k = 0.15$ and 0.095 at 283 K for R = methyl, isopropyl respectively) are very similar to those for our molybdenum complexes and entropies of activation for the reaction are large and negative, also suggesting a twist mechanism for this isomerization reaction.¹³

(23) Bond, A. M.; Grabaric, B. S.; Grabaric, Z. *Inorg. Chem.* **1978**, *17*, 1013.

Conclusions

Investigations of the cyclic voltammetry of the series of complexes $Mo(CO)_{6-n}(dmpi)_n$ support the principle of ligand additivity, and an E_L value of 0.43 has been calculated for the *dmpi* ligand. Removal of one electron to form the cation becomes successively easier because more *dmpi* ligands are substituted for carbonyls, as borne out by molecular orbital calculations. In two members of the series, $n = 3$ and 4, two isomers have been observed and their unique oxidation potentials measured. The *mer*- $Mo(CO)_3(dmpi)_3$ complex is easier to oxidize than the *fac*, and similarly, the *trans*- $Mo(CO)_2(dmpi)_4$ complex is easier to oxidize than the *cis*. These isomers have not been isolated but are observed voltammetrically, and their identities have been confirmed in infrared spectroelectrochemistry experiments. From digital simulation of the cyclic voltammetry, the rate constants for the four isomerization reactions have been determined.

Acknowledgment. The FTIR used to perform the spectroelectrochemistry experiments was purchased in part with funds provided by NSF Grant USE-8951598 (D.C.B.) and the computer equipment for the molecular orbital calculations was purchased from funds provided by NSF-ILI Grant USE-9252169. This research was supported by the NSF-REU (S.L.P., Grant CHE-9001332), Research Corp. (L.J.L., Grant C-3354), and the UST Faculty Development Committee (D.C.B.). L.J.L and S.L.P. thank Professor Martin Minelli for providing $Mo(CO)_4(dmpi)_2$, $Mo(CO)_3(dmpi)_3$, $Mo(CO)_5(dmpi)$ and for helpful discussions.

Supplementary Material Available: Figures of the IRSEC for the oxidation of *fac*- $Mo(CO)_3(dmpi)_3$ and digital simulation of the oxidative voltammetry of *cis*- $Mo(CO)_2(dmpi)_4$ at 0.075 V/s (2 pages). Ordering information is given on any current masthead page.

IC931245Y